Journal of the Serbian Chemical Society
JSCS-info@shd.org.rs • www.shd.org.rs/JSCS
J. Serb. Chem. Soc. *82* (12) 1433–1444 (2017)
JSCS–5051
UDC 546.873–31+546.815–31:543.57:544.015.3
Original scientific paper

Investigation of Bi_2O_3-rich part of Bi_2O_3–PbO phase diagram

ALEKSANDRA DAPČEVIĆ[1]*[#], DEJAN POLETI[1#], LJILJANA KARANOVIĆ[2] and JELENA MILADINOVIĆ[3]

[1]*University of Belgrade, Department of General and Inorganic Chemistry, Faculty of Technology and Metallurgy, Karnegijeva 4, 11000 Belgrade, Serbia,* [2]*University of Belgrade, Laboratory of Crystallography, Faculty of Mining and Geology, Đušina 7, 11000 Belgrade, Serbia and* [3]*University of Belgrade, Department of Inorganic Chemical Technology, Faculty of Technology and Metallurgy, Karnegijeva 4, 11000 Belgrade, Serbia*

(Received 11 July, revised 12 October, accepted 16 October 2017)

Abstract: A new Bi-rich part of Bi_2O_3–PbO phase diagram was determined using differential thermal analysis and X-ray powder diffraction techniques. Four solid solutions, α-Bi_2O_3, γ-Bi_2O_3, δ-Bi_2O_3 and β_{ss}-$Bi_8Pb_5O_{17}$, can be distinguished below 37.5 mol % of PbO and one compound, β_2-$Bi_8Pb_5O_{17}$. Two of them, δ-Bi_2O_3 and β_{ss}-$Bi_8Pb_5O_{17}$ are high-temperature phases. The large field of γ-Bi_2O_3 stability was implemented making the crucial difference comparing to phase diagrams from the Bi_2O_3–PbO system published so far.

Keywords: Bi_2O_3; PbO; phase diagram.

INTRODUCTION

Bismuth(III) oxide is a multimorphic material with seven structural modifications where the monoclinic α-Bi_2O_3 is stable, tetragonal β-, body-centered cubic γ- and orthorhombic ε-Bi_2O_3 are metastable, the face-centred cubic δ-Bi_2O_3 is a high-temperature polymorph, the η-Bi_2O_3 is a high-pressure phase, while ω-Bi_2O_3 is observed as a thin film only.[1–13] The synthetic conditions and the presence of dopants determine which modification will be obtained. Pb^{2+} is an interesting choice of dopant because various PbO-doped Bi_2O_3-based phases show the extraordinary characteristics: they are wide-band gap high-resistivity semi-insulating, photoconductive, photoluminescent, electronic, optoelectronic, acoustic and piezoelectric materials, good high-temperature ionic conductors, but also exhibit mixed ionic/electronic conductivity that could be useful in the oxygen selective membranes.[14–22] Moreover, the mixed heavy metal oxide glasses based on Bi_2O_3 and PbO have interesting physical properties such as high density, high linear or

* Corresponding author. E-mail: hadzi-tonic@tmf.bg.ac.rs
[#] Serbian Chemical Society member.
https://doi.org/10.2298/JSC170711111D

non-linear refractive index and long infrared cut-off.[23–27] Within Bi_2O_3–PbO system a great number of phases (α-Bi_2O_3, β-Bi_2O_3, γ-Bi_2O_3, δ-Bi_2O_3, γ-$Bi_{12}PbO_{19}$, β_1-$BiPbO_{11}$, β_2-$Bi_8Pb_5O_{17}$, β_3-$Bi_{1.23}Pb_{0.77}O_{2.62}$, φ-$Bi_8Pb_5O_{17}$, β-$Bi_8Pb_5O_{17}$, $Bi_2Pb_3O_6$, γ-PbO) with different Bi/Pb ratio and thermal history have been reported.[28] The conditions (temperature and concentration) for a synthesis of specific phase can be predicted from Bi_2O_3–PbO phase diagrams.[29–31]

The Bi_2O_3–PbO phase diagram was firstly established by Belladen[29] who described Bi_8PbO_{13}, $Bi_6Pb_2O_{11}$ and $Bi_2Pb_2O_5$ compounds. Later, Boivin and Tridot[30] presented their data for the same system finding $Bi_{12}PbO_{19}$ (known also as γ-Bi_2O_3 phase with sillenite-like structure), $Bi_6Pb_2O_{11}$, $Bi_8Pb_5O_{17}$, $Bi_2Pb_3O_6$, $Bi_6Pb_7O_{16}$ and β_{ss}-$Bi_8Pb_5O_{17}$. The most detailed Bi_2O_3–PbO phase diagram was published by Biefeld and White[31] representing the improvement of the one reported by Boivin and Tridot[30]. They confirmed the existence of $Bi_{12}PbO_{19}$, $Bi_6Pb_2O_{11}$, $Bi_8Pb_5O_{17}$, $Bi_2Pb_3O_6$ and β_{ss}-$Bi_8Pb_5O_{17}$ but they did not detect $Bi_6Pb_7O_{16}$. Later works on the Bi_2O_3–PbO system of Zhongbao *et al.*[32], Braileanu *et al.*[33], Ganesan *et al.*[34] and Diop *et al.*[35] mostly confirmed the results of Biefeld and White.[31]

Regarding previously mentioned properties and the wide area of possible applications of Bi_2O_3 doped with PbO, our research group was particularly oriented toward the Bi-rich part of the Bi_2O_3–PbO phase diagram. Therefore, 37.5 mol % of PbO was appropriately set to be the upper limit of the dopant concentration. According to Biefeld and White[31], this part of diagram could be divided in three regions based on phase composition at room temperature: the region with less than 14.3 mol % PbO and coexistence of α- and γ-Bi_2O_3 phases, the region containing exactly 14.3 mol % PbO and only single-phase γ-Bi_2O_3 (labeled as $Bi_{12}PbO_{19}$ by authors), and the region with more than 14.3 mol % PbO and coexistence of γ-Bi_2O_3 and $Bi_8Pb_5O_{17}$. In the phase diagram[31] three solid solutions can be distinguished below 37.5 mol % of PbO, α-Bi_2O_3, δ-Bi_2O_3 and high-temperature β_{ss}-$Bi_8Pb_5O_{17}$ (denoted as β by authors) and two compounds, γ-Bi_2O_3 and $Bi_8Pb_5O_{17}$, which was later described as a phase with at least three low-temperature polymorphs: β_1-$Bi_8Pb_5O_{17}$, β_2-$Bi_8Pb_5O_{17}$ and φ-$Bi_8Pb_5O_{17}$[34]. Namely, it was at first recognized that, depending on PbO content, the rapid cooling of β_{ss}-$Bi_8Pb_5O_{17}$ could result in forming of monoclinic β_1-$Bi_8Pb_5O_{17}$ or tetragonal β_2-Bi8Pb5O$_{17}$.[22] However, according to Fee *et al.*[21], this tetragonal β_2-$Bi_8Pb_5O_{17}$ phase is formed only if the mixture having $Bi_8Pb_5O_{17}$ nominal composition is heated below 470 or above 590 °C. But, if some material with composition $Bi_8Pb_5O_{17}$ is reheated to any temperature belonging to 470–590 °C interval, triclinic φ-$Bi_8Pb_5O_{17}$ phase appears upon cooling.

During our study on the Bi_2O_3 doped with various dopants a large number of new γ-Bi_2O_3 phases were already synthesized using different methods.[36–39] The earlier investigation[36] based on γ-Bi_2O_3 with the composition $(Bi_{23.68}Pb_{0.32})(Bi_{1.28}Pb_{0.72})O_{38.48}$ emphasized the distinction of the Bi_2O_3–PbO

system from the structural point of view and possible Bi^{3+}–Pb^{2+} cation exchange, due to the similarity of Bi^{3+} and Pb^{2+}: they are isoelectronic, with similar ionic radii and both have the lone electron pair. Therefore, there are a lot of possible solid solutions in the Bi_2O_3–PbO system. Since the application strongly depends on properties, it is very important to know the exact conditions under which a specific phase from this system can be obtained. In that sense, it is well established that the Bi_2O_3–PbO phase diagram is crucial.

In this article, in order to improve the existing Bi_2O_3–PbO phase diagrams, the high temperature treatment of eleven pseudo-binary Bi_2O_3–PbO mixtures in the Bi-rich (x(PbO) ≤ 37.5 mol %) region, as well as the final phase composition and thermal behaviour of obtained products are reported. Seven final mixtures represent the single-phase and four are two-phase samples. The effects of temperature and dopant amount on synthesis are discussed.

EXPERIMENTAL

Eleven pseudo-binary Bi_2O_3–PbO mixtures with different oxide proportions (Table I) were prepared from bismite, α-Bi_2O_3 (99.975 %, Alfa Aesar) and massicot, PbO (99.9%, Alfa Aesar). The starting components were dryly homogenized for about 30 min in an agate mortar, heated at 690 °C for 1.5 h (heating rate 4 °C/min) in an open Pt crucible and then slowly cooled to room temperature. Afterward the samples were reground and examined on a Philips PW1710 X-ray powder diffractometer (XRD) using monochromatic Cu $K\alpha$ radiation (λ = 1.5418 Å) and the step-scan mode (2θ range was from 4 to 90°, step width 0.02°, time per step 0.5 s). Depending on the phase composition some samples were additionally thermally treated for 1.5 and 3 h at 690 °C and further, if necessary, at 750 °C. The treatments were considered as finished if two simultaneous XRD patterns did not show any significant differences. The unit cell parameters were calculated by the least-squares method using the LSUCRIPC program.[40] The software PowderCell[41] was used for the determination of an approximate phase ratio in a Rietveld-like refinement. The differential thermal analysis (DTA) was carried out on an SDT Q600 instrument (TA Instruments) in N_2 atmosphere (flow rate: 100 cm^3 min^{-1}; heating rate: 20 °C min^{-1}). Since no significant thermal effects were observed below 400 °C, the selected products or initial mixtures were analyzed cyclically ranging from 400 to 900 °C.

RESULTS AND DISCUSSION

As given in Table I, after the thermal treatment of $Bi_{12}Pb_{0.16}O_{18.16}$, *i.e.*, the sample with the highest Bi content, the presence of α-Bi_2O_3 (PDF #41-1449) phase was found besides Pb-doped γ-Bi_2O_3 (PDF #84-0831). This means that the PbO content was obviously too low to induced transformation of all α-Bi_2O_3 into the γ-Bi_2O_3 phase (Fig. 1a). The single-phase Pb-doped γ-Bi_2O_3 has been obtained from next seven starting mixtures, *i.e.*, in approximately 5–17 mol % PbO. As an illustration, one of the corresponding powder patterns is shown in Fig. 1b. The increased dopant content of more than about 20 mol % resulted in the formation of a lead-rich phase, β_2-$Bi_8Pb_5O_{17}$ (PDF #41-0405) besides Pb-doped γ-Bi_2O_3 (Fig. 1c). However, no matter whether a single or multiphase

sample was obtained, the unit cell parameters of all Pb-doped γ-Bi_2O_3 were in a narrow 10.24–10.27 Å range. The fact that the single-phase Pb-doped γ-Bi_2O_3 was obtained within such broad range of Pb concentrations confirmed the implied Bi^{3+}–Pb^{2+} ion isomorphous replacement, which is completely in accordance with our earlier results.[36] According to Zyryanov[42], Bi^{3+}–Pb^{2+} ion exchange can be extended by mechanochemical synthesis, allowing the preparation of Pb-doped single-phase γ-Bi_2O_3 even from $2Bi_2O_3$·PbO and Bi_2O_3·PbO starting mixtures. This, however, can be explained by the nature of mechanochemical treatments, which easily result in metastable or unstable products. On the contrary, in the Bi_2O_3–PbO phase diagram established by Biefeld and White[31], there is only one composition corresponding to the single γ-Bi_2O_3 phase: $Bi_{12}PbO_{19}$ (14.3 mol % of PbO) standing as a single line.

TABLE I. Heat treatment, phase composition and Pb-doped γ -Bi_2O_3 unit cell parameters of obtained samples

Nominal composition	PbO content mol %	Time, h/ Temperature, °C	Phase composition wt. %	Unit cell parameter of γ-Bi_2O_3 phase, *a* / Å
$Bi_{12}Pb_{0.16}O_{18.16}$	2.6	3/750	γ-Bi_2O_3 (14) + α-Bi_2O_3 (86)	10.241(4)
$Bi_{12}Pb_{0.32}O_{18.32}$	5.1	3/750	γ-Bi_2O_3	10.255(1)
$Bi_{12}Pb_{0.33}O_{18.33}$	5.3	1.5/690	γ-Bi_2O_3	10.258(1)
$Bi_{12}Pb_{0.50}O_{18.50}$	7.7	1.5/690	γ-Bi_2O_3	10.254(2)
$Bi_{12}Pb_{0.81}O_{18.81}$	11.9	1.5/690	γ-Bi_2O_3	10.267(1)
$Bi_{12}PbO_{19}$	14.3	1.5/690	γ-Bi_2O_3	10.260(1)
$Bi_{12}Pb_{1.09}O_{19.09}$	15.4	3/750	γ-Bi_2O_3	10.2696(7)
$Bi_{12}Pb_{1.20}O_{19.20}$	16.7	3/690	γ-Bi_2O_3	10.2652(5)
$Bi_{12}Pb_{1.50}O_{19.50}$	20.0	3/690	γ-Bi_2O_3 (90) + β_2-$Bi_8Pb_5O_{17}$ (10)	10.2656(7)
$Bi_{12}Pb_{2.18}O_{20.18}$	26.6	1.5/690	γ-Bi_2O_3 (82) + β_2-$Bi_8Pb_5O_{17}$ (18)	10.2615(8)
$Bi_{12}Pb_{3.60}O_{21.60}$	37.5	1.5/690	γ-Bi_2O_3 (62) + β_2-$Bi_8Pb_5O_{17}$ (38)	10.257(1)

Taking into account the XRD results, we can distinguish three regions of the final phase composition: region A for $x < 5.1$ mol % PbO with the coexisting α- and γ-Bi_2O_3 phases, region B for $5.1 \leq x \leq 16.7$ mol % PbO with the single-phase γ-Bi_2O_3, and region C for $16.7 < x \leq 37.5$ mol % PbO with the coexistence of γ-Bi_2O_3 and β_2-$Bi_8Pb_5O_{17}$. The main difference between these regions and those reported in phase diagram[31] is the existence of broad B region of γ-Bi_2O_3 single-phase comparing to the mentioned single line corresponding to γ-Bi_2O_3 with $Bi_{12}PbO_{19}$ composition and, as a consequence, the narrower A and C regions.

The results obtained from the cyclic DTA curves (the representative ones are shown in Fig. 2) are summarized in Table II. The experimentally determined temperatures are assigned to the phase transitions according to the corresponding ones

found in Bi_2O_3–PbO phase diagram.[31] The thermal behaviour can be discussed within the same three regions obtained from XRD results, *i.e.*, A, B and C.

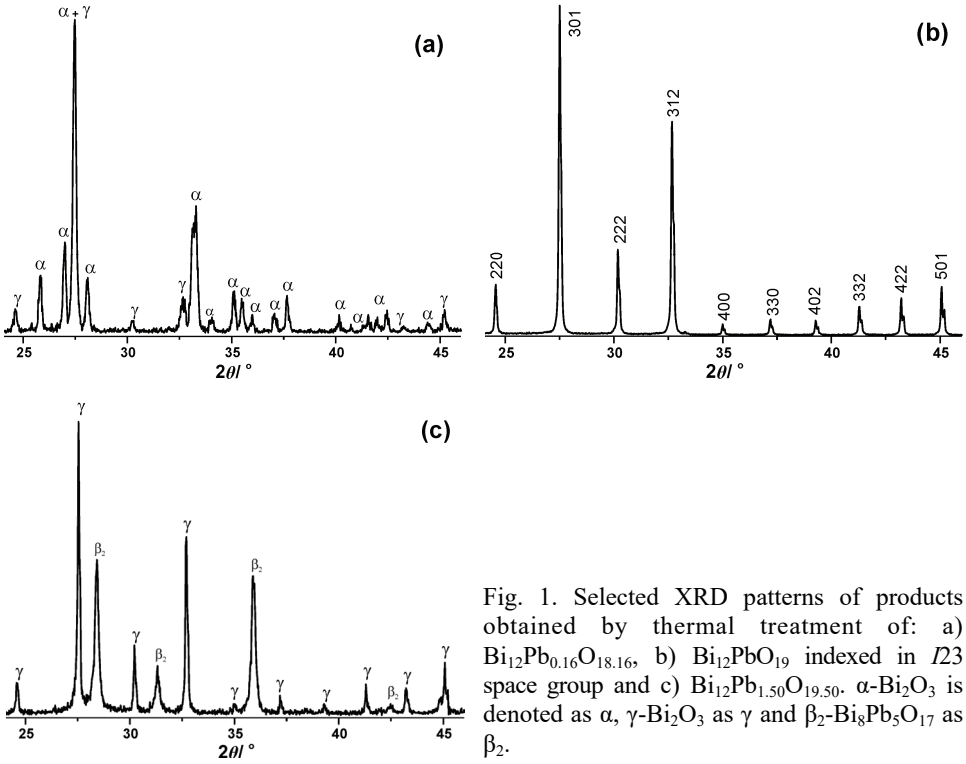

Fig. 1. Selected XRD patterns of products obtained by thermal treatment of: a) $Bi_{12}Pb_{0.16}O_{18.16}$, b) $Bi_{12}PbO_{19}$ indexed in *I*23 space group and c) $Bi_{12}Pb_{1.50}O_{19.50}$. α-$Bi_2O_3$ is denoted as α, γ-Bi_2O_3 as γ and β_2-$Bi_8Pb_5O_{17}$ as β_2.

When $Bi_{12}Pb_{0.16}O_{18.16}$ sample is heated (Fig. 2a), α-Bi_2O_3 + γ-Bi_2O_3 → α-Bi_2O_3 + δ-Bi_2O_3 → δ-Bi_2O_3 transitions occur at 709 and 730 °C, respectively (Table II). These temperatures are in agreement with the values for same transitions reported by Biefeld and White[31]. The melting and crystallization points (824 and 817 °C, respectively) are also consistent. The small hysteresis of about 7 °C is found for the melting-crystallization processes. On cooling, only δ-Bi_2O_3 → α-Bi_2O_3 + γ-Bi_2O_3 transition takes place after the crystallization. Both processes occur at temperatures that correspond well to those found in the phase diagram.[31] The later transition happens in several close steps probably due to δ-Bi_2O_3 → α-Bi_2O_3 + δ-Bi_2O_3 → α-Bi_2O_3 → α-Bi_2O_3 + γ-Bi_2O_3.

The existence of the single-phase Pb-doped γ-Bi_2O_3 within a broad field (5.1–16.7 mol % of PbO, *i.e.*, 37.5–10.0 Bi/Pb ratio) is the main characteristic of the region B. The very small endothermic peaks precede the γ-Bi_2O_3 → δ-Bi_2O_3 transition indicating the presence of traces of α-Bi_2O_3 phase in the samples with up to about 8 mol % PbO. These traces of α-Bi_2O_3 phase were not detected in XRD patterns. The melting points are in the range from 777 to 815 °C (Table II)

which is in excellent agreement with those found in the phase diagram[31]. Both, the melting and crystallization temperatures increase with the dopant content decreasing. The crystallization points are at slightly lower temperatures than in the phase diagram[31] causing smaller hysteresis. Except for $Bi_{12}Pb_{1.20}O_{19.20}$, the crystallization occurs in one step for all the samples. This exception is probably related to the formation of the negligible amount of another crystalline phase. The only comparison of temperatures for δ-$Bi_2O_3 \rightarrow \gamma$-$Bi_2O_3$ phase transition could be made for the $Bi_{12}PbO_{19}$ sample since that composition correspond to the only single γ-Bi_2O_3 phase in the existing phase diagram.[31] We obtained the significantly lower temperature (573 *vs.* 715 °C) which is due to the thermal history[13] and will be explained later using DTA of the starting mixture and not the final product.

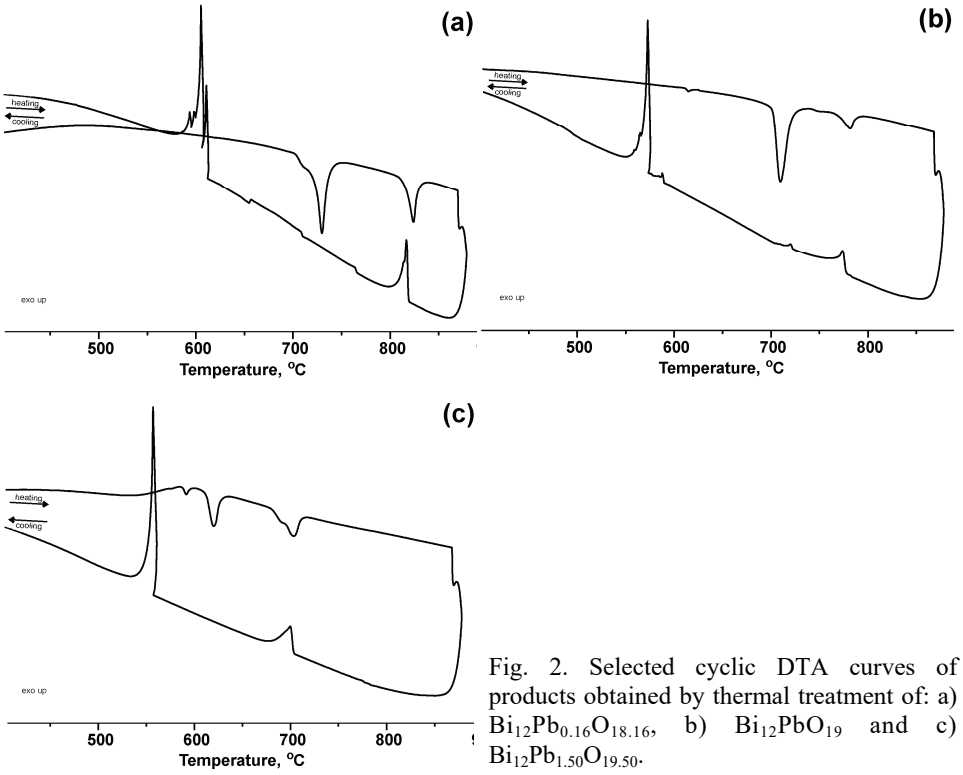

Fig. 2. Selected cyclic DTA curves of products obtained by thermal treatment of: a) $Bi_{12}Pb_{0.16}O_{18.16}$, b) $Bi_{12}PbO_{19}$ and c) $Bi_{12}Pb_{1.50}O_{19.50}$.

According to the phase diagram,[31] the temperatures of first two transitions within region C, γ-Bi_2O_3 + β_2-$Bi_8Pb_5O_{17} \rightarrow \gamma$-$Bi_2O_3$ + $Bi_6Pb_2O_{11} \rightarrow \gamma$-$Bi_2O_3$ + β_{ss}-$Bi_8Pb_5O_{17}$, are independent of the dopant content. The temperatures of these transitions (Table II) obtained by the thermal analysis of $Bi_{12}Pb_{1.50}O_{19.50}$ (Fig. 2c), $Bi_{12}Pb_{2.18}O_{20.18}$ and $Bi_{12}Pb_{3.60}O_{21.60}$ are also independent of dopant content, but

TABLE II. The temperatures of phase transitions determined from DTA of final products; labels: α stands for α-Bi_2O_3, γ for γ-Bi_2O_3, δ for δ-Bi_2O_3, β_2 for β_2-$Bi_8Pb_5O_{17}$, BPO for $Bi_6Pb_2O_{11}$, βss for βss-$Bi_8Pb_5O_{17}$ and L for liquid

Nominal composition	PbO mole ratio mol %	Phase composition, wt. %	Phase transition temperature, °C											
			Heating								Cooling			
			α+γ ↓ α+δ	α+δ ↓ δ	γ ↓ δ	γ+β_2 ↓ γ+BPO	γ+BPO ↓ γ+β_{ss}	γ+β_{ss} ↓ δ+β_{ss}	γ+β_{ss} ↓ β_{ss}	Melting	L ↓ δ	δ ↓ α+γ	δ ↓ γ	δ ↓ γ+β_2
$Bi_{12}Pb_{0.16}O_{18.16}$	2.6	γ-Bi_2O_3 (14) + α-Bi_2O_3 (86)	709	730						824	817	605		
$Bi_{12}Pb_{0.32}O_{18.32}$	5.1	γ-Bi_2O_3			703, 722					815	809		597	
$Bi_{12}Pb_{0.33}O_{18.33}$	5.3	γ-Bi_2O_3			696, 717					807	799		582	
$Bi_{12}Pb_{0.50}O_{18.50}$	7.7	γ-Bi_2O_3			701, 716					806	799		582	
$Bi_{12}Pb_{0.81}O_{18.81}$	11.9	γ-Bi_2O_3			714					782	755		550	
$Bi_{12}PbO_{19}$	14.3	γ-Bi_2O_3			710					782	774		573	
$Bi_{12}Pb_{1.09}O_{19.09}$	15.4	γ-Bi_2O_3			711					777	771		664	
$Bi_{12}Pb_{1.20}O_{19.20}$	16.7	γ-Bi_2O_3			709					778	770, 729		663	
$Bi_{12}Pb_{1.50}O_{19.50}$	20.0	γ-Bi_2O_3 (90) + β_2-$Bi_8Pb_5O_{17}$ (10)				589	615	710		732, 758	753, 724			574
$Bi_{12}Pb_{2.18}O_{20.18}$	26.6	γ-Bi_2O_3 (82) + β_2-$Bi_8Pb_5O_{17}$ (18)				591	615	709		728	721, 728			563
$Bi_{12}Pb_{3.60}O_{21.60}$	37.5	γ-Bi_2O_3 (62) + β_2-$Bi_8Pb_5O_{17}$ (38)				592	620		691	704	700			557

slightly different than those from the phase diagram[31]. The transitions γ-Bi_2O_3 + β_{ss}-$Bi_8Pb_5O_{17}$ → δ-Bi_2O_3 + β_{ss}-$Bi_8Pb_5O_{17}$ for $Bi_{12}Pb_{1.50}O_{19.50}$ and $Bi_{12}Pb_{2.18}O_{20.18}$, as well as γ-$Bi_2O_3$ + β_{ss}-$Bi_8Pb_5O_{17}$ → β_{ss}-$Bi_8Pb_5O_{17}$ for $Bi_{12}Pb_{3.60}O_{21.60}$ occur at temperatures 10–20 °C lower than the corresponding ones found in the phase diagram[31], but the melting and the crystallization temperatures are in accordance with the same Bi_2O_3–PbO phase diagram. The extremely small hysteresis of only few °C is characteristic for these processes.

In order to determine the field of stability of γ-Bi_2O_3, the additional DTA below melting process were performed on three starting mixtures (Fig. 3, Table III). The $Bi_{12}Pb_{1.20}O_{19.20}$, $Bi_{12}Pb_{0.32}O_{18.32}$ and $Bi_{12}PbO_{19}$ were chosen since the first two are at the borderlines for synthesis of single-phase γ-Bi_2O_3, while the third one is taken as only one composition comparable with the Bi_2O_3–PbO phase diagram.[31] On heating, all three α-Bi_2O_3/PbO mixtures transform primarily to the α-Bi_2O_3/γ-Bi_2O_3 mixture, which converts to δ-Bi_2O_3 phase through two following transitions α-Bi_2O_3 + γ-Bi_2O_3 → γ-Bi_2O_3 + δ-Bi_2O_3 → δ-Bi_2O_3. On cooling, only δ-Bi_2O_3 → γ-Bi_2O_3 transition takes place. This transition for $Bi_{12}PbO_{19}$ sample occurs at temperature closer to that of the corresponding transition in the DTA existing phase diagram[31] than to the one obtained from the DTA of final products. This is another confirmation that the thermal history could have an influence on temperature of a phase transition.[13]

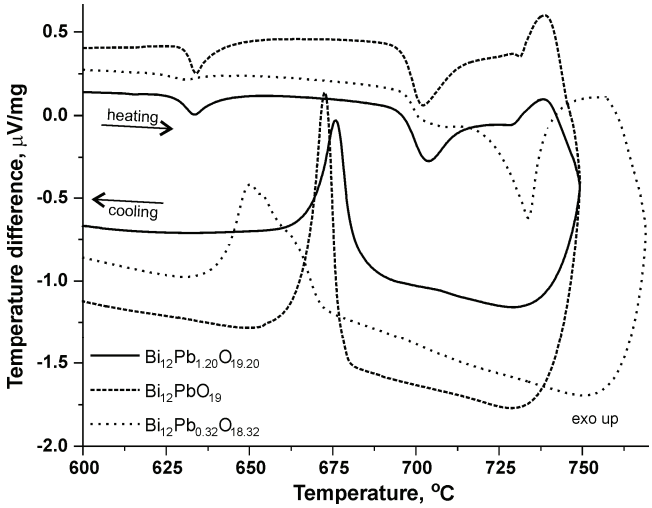

Fig. 3. Cyclic DTA curves of selected starting mixtures.

The temperatures of δ-Bi_2O_3 → γ-Bi_2O_3 transition of all three systems analyzed from the starting mixture were taken as temperature boundaries for the formation and stability of the γ-Bi_2O_3. This field of γ-Bi_2O_3 stability is not present in the earlier published Bi_2O_3–PbO phase diagrams,[29-31] but according to our

results we assume that this field does exist as well as the areas of γ- and δ-Bi_2O_3 coexistence. Such two-phase fields that should be between areas of γ-Bi_2O_3 and δ-Bi_2O_3 stability also do not exist in the phase diagram[31] but there are two undefined fields, which are probably related to the coexistence of γ- and δ-Bi_2O_3.

Table III. The temperatures of phase transitions determined from DTA of some starting mixtures; labels: α stands for α-Bi_2O_3, γ for γ-Bi_2O_3 and δ for δ-Bi_2O_3

Nominal composition	PbO content mol %	Phase composition	Phase transition temperature, °C			
			Heating		Cooling	
			α + PbO → α + γ	α + γ → γ + δ	γ + δ → δ	δ → γ
$Bi_{12}Pb_{0.32}O_{18.32}$	5.1	γ-Bi_2O_3	631	704	734	652
$Bi_{12}PbO_{19}$	14.3	γ-Bi_2O_3	634	703	731	672
$Bi_{12}Pb_{1.20}O_{19.20}$	16.7	γ-Bi_2O_3	634	703	731	676

The temperatures of the determined phase transitions as well as the experimentally found field of γ-Bi_2O_3 stability were incorporated in the Bi_2O_3–PbO phase diagram[31] (Fig. 4a). Based on the given results and taking into account the rules for construction of a phase diagram,[43] the new Bi_2O_3-rich part of Bi_2O_3––PbO phase diagram is proposed (Fig. 4b).

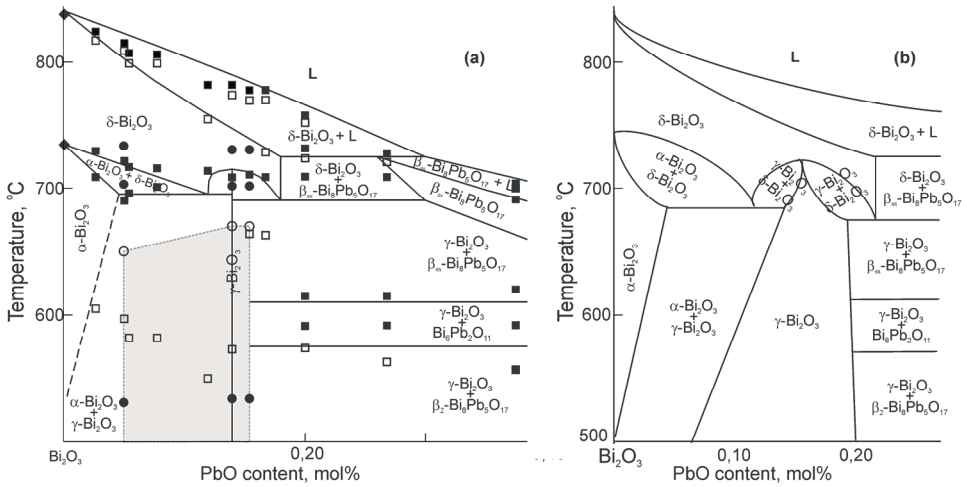

Fig. 4. a) Field of γ-Bi_2O_3 stability (grey) in Bi_2O_3–PbO phase diagram.[31] The labels for phases are set to be up to date not being identical to those used by Biefeld and White.[31] The following symbols are used for: ■ – temperatures of phase transitions recorded on heating of final products, □ – temperatures of phase transitions recorded on cooling of final products, ● – temperatures of phase transitions recorded on heating of starting mixtures, ○ – temperatures of phase transitions recorded on cooling of starting mixtures, ◆ – temperatures of phase transitions recorded on heating of α-Bi_2O_3 phase. b) Proposition of Bi_2O_3-rich part of Bi_2O_3–PbO phase diagram.

Contrary to Biefeld and White[31] four solid solutions were found: α-Bi_2O_3, γ-Bi_2O_3, δ-Bi_2O_3 and β_{ss}-$Bi_8Pb_5O_{17}$ and one compound, β_2-$Bi_8Pb_5O_{17}$. Among them, α-Bi_2O_3, γ-Bi_2O_3 and β_2-$Bi_8Pb_5O_{17}$ are low temperature phases. No eutectic was observed within Bi_2O_3-rich region but two eutectoids, both involving γ-Bi_2O_3, are distinctive, one at about 12 mol % of PbO and 695 °C (δ-Bi_2O_3 → γ-Bi_2O_3 + α-Bi_2O_3) and another at about 22 mol % of PbO and 690 °C (δ-Bi_2O_3 → γ-Bi_2O_3 + β_{ss}-$Bi_8Pb_5O_{17}$). The divergences between our results and those of Biefeld and White[31] are difficult to explain from the experimental point of view, because of the lack of experimental details in the paper.[31] For example, there is no information on the DTA purge flow or atmosphere. The only known difference is the heating rate but Biefeld and White[31] had determined that this parameter had no influence on the results. In that sense, we believe that the established differences could be the consequence of more precise measurements.

CONCLUSION

This work represents a contribution to the examination of Bi_2O_3–PbO system in the Bi_2O_3-rich region. The correct phase diagram is important in order to conduct a high-temperature synthesis of a concrete compound suitable for desired application. In that sense, we proposed a new Bi-rich part of Bi_2O_3–PbO phase diagram that differs from Bi-rich region of the phase diagrams published by now. In other to obtain the structural characterization of all phases, our future investigations will be directed towards the confirmation of these results by using the high-temperature X-ray powder diffraction.

Acknowledgement. The authors gratefully acknowledge the financial support of the Ministry of Education, Science and Technological Development of the Republic of Serbia (Grant No. III 45007).

ИЗВОД

ИСПИТИВАЊЕ ФАЗНОГ ДИЈАГРАМА Bi_2O_3–PbO У ОБЛАСТИ БОГАТОЈ БИЗМУТ(III)-ОКСИДОМ

АЛЕКСАНДРА ДАПЧЕВИЋ[1], ДЕЈАН ПОЛЕТИ[1], ЉИЉАНА КАРАНОВИЋ[2] и ЈЕЛЕНА МИЛАДИНОВИЋ[3]

[1]Универзитет у Београду, Катедра за општу и неорганску хемију, Технолошко–металуршки факултет, Карнегијева 4, 11000 Београд, [2]Универзитет у Београду, Лабораторија за кристалографију, Рударско–геолошки факултет, Ђушина 7, 11000 Београд и [3]Универзитет у Београду, Катедра за неорганску хемијску технологију, Технолошко–металуршки факултет, Карнегијева 4, 11000 Београд

Применом метода диференцијалне термијске анализе и рендгенске дифракције микрокристалних узорака, одређена је нова бизмутом богата област у фазном дијаграму Bi_2O_3–PbO. У области концентрација мањим од 37,5 mol % PbO, пронађена су четири чврста раствора: α-Bi_2O_3, γ-Bi_2O_3, δ-Bi_2O_3 и β_{ss}-$Bi_8Pb_5O_{17}$, и једно једињење: β_2-$Bi_8Pb_5O_{17}$. Од свих наведених, δ-Bi_2O_3 и β_{ss}-$Bi_8Pb_5O_{17}$ су високотемпературне фазе. Највећу разлику у односу на фазне дијаграме објављене до сада за систем Bi_2O_3–PbO, чини постојање велике области стабилности фазе γ-Bi_2O_3.

(Примљено 11.јула, ревидирано 12. октобра, прихваћено 16. октобра 2017)

REFERENCES

1. S. F. Radaev, V. I. Simonov, Yu. F. Kargin, *Acta Crystallogr., B* **48** (1992) 604
2. H. A. Harwig, *Z. Anorg. Allg. Chem.* **444** (1978) 151
3. H. A. Harwig, A. G. Gerards, *Thermochim. Acta* **28** (1979) 121
4. H. A. Harwig, J. W. Weenk, *Z. Anorg. Allg. Chem.* **444** (1978) 167
5. E. M. Levin, R. S. Roth, *J. Res. Nat. Bur. Stand., A* **68** (1964) 189
6. N. M. Sammes, G. A. Tompsett, H. Näfe, F. Aldinger, *J. Eur. Ceram. Soc.* **19** (1999) 1801
7. L. G. Sillén, *Ark. Kemi Mineral. Geol., A* **12** (1937) 1
8. G. Gattow, H. Schröder, *Z. Anorg. Allg. Chem.* **318** (1962) 176
9. N. Cornei, N. Tancret, F. Abraham, O. Mentre, *Inorg. Chem.* **45** (2006) 4886
10. A. F. Gualtieri, S. Imovilli, M. Prudenziati, *Powder Diffr.* **12** (1997) 90
11. S. Ghedia, T. Locherer, R. Dinnebier, D. L. V. K. Prasad, U. Wedig, M. Jansen, A. Senyshyn, *Phys. Rev., B* **82** (2010) 1
12. T. Atou, H. Faqir, M. Kikuchi, H. Chiba, Y. Syono, *Mater. Res. Bull.* **33** (1998) 289
13. M. Drache, P. Roussel, J-P. Wignacourt, *Chem. Rev.* **107** (2007) 80
14. M. Valant, D. Suvorov, *J. Am. Ceram. Soc.* **84** (2001) 2900
15. M. Valant, D. Suvorov, *Chem. Mater.* **14** (2002) 3471
16. M. T. Borowiec, B. Kozankiewicz, H. Szymczak, J. Zmija, A. Majchrowski, M. Zaleski, T. Zayarnyuk, *Acta. Phys. Pol., A* **96** (1999) 785
17. T. Mitsuyu, K. Wasa, S. Hayakawa, *J. Appl. Phys.* **47** (1976) 2901
18. N. M. Sammes, G. Tompsett, A. M. Cartner, *J. Mater. Sci.* **30** (1995) 4299
19. M. Manier, J. C. Champarnaud-Mesjard, J. P. Mercurio, D. Bernache, B. Frit, *Mater. Chem. Phys.* **19** (1988) 167
20. M. G. Fee, N. J. Long, *Solid State Ionics* **86**–**88** (1996) 733
21. M. G. Fee, N. M. Sammes, G. Tomsett, T. Soto, A. M. Cartner, *Solid State Ionics* **95** (1997) 183
22. F. Honnart, J. C. Boivin, D. Thomas, K. J. De Vries, *Solid State Ionics* **9**–**10** (1983) 921
23. K. Knoblochova, H. Ticha, J. Schwarz, L. Tichy, *Opt. Mater.* **31** (2009) 895
24. A. Pan, A. Ghosh, *J. Non-Cryst. Solids* **271** (2000) 157
25. A. H. Reshak, G. Lakshminarayana, G. Proskurina, V. G. Yushanin, S. Calus, M. Chmiel, R. Miedzinski, M. G. Brik, *Opt. Commun.* **283** (2010) 3049
26. S. M. Salem, E. A. Mohamed, *J. Non-Cryst. Solids* **357** (2011) 1153
27. D. M. Shi, Q. Qian, *Physica, B* **405** (2010) 2503
28. Y. Zhang, N. Sammes, Y. Du, *Solid State Ionics* **124** (1999) 179
29. L. Belladen, *Gazz. Chim. Ital.* **52** (1922) 160
30. J. C. Boivin, G. Tridot, *C. R. Acad. Sci.* **C278** (1974) 865
31. R. M. Biefeld, S. S. White, *J. Am. Ceram. Soc.* **64** (1981) 182
32. S. Zhongbao, L. Kuiren, M. Bo, L. Ying, Y. Yang, *J. Inorg. Mater.* **11** (1996) 570
33. A. Braileanu, M. Zaharescu, D. Crisan, E. Segal, *J. Therm. Anal.* **49** (1997) 1197
34. R. Ganesan, T. Gnanasekaran, R. S. Srinivasa, *J. Nucl. Mater.* **375** (2008) 229
35. I. Diop, N. David, J. M. Fiorani, R. Podor, M. Vilasi, *J. Chem. Thermodyn.* **41** (2009) 420
36. A. Dapčević, D. Poleti, Lj. Karanović, *Powder Diffr.* **27** (2012) 2
37. D. Poleti, Lj. Karanović, M. Zdujić, Č. Jovalekić, Z. Branković, *Solid State Sci.* **6** (2004) 239
38. D. Poleti, Lj. Karanović, A. Hadži-Tonić, *Z. Kristallogr.* **222** (2007) 59.
39. A. Dapčević, D. Poleti, Lj. Karanović, J. Rogan, G. Dražić, *Solid State Sci.* **25** (2013) 93
40. R. G. Garwey, *Powder Diffr.* **1** (1986) 114

41. W. Kraus, G. Nolze, PowderCell for Windows, V.2.4, Federal Institute for Materials Research and Testing, Berlin, Germany
42. V. V. Zyryanov, *J. Struct. Chem.* **45** (2004) 454
43. J. C. Zhao, *Methods for Phase Diagram Determination*, Elsevier Science, Amsterdam, 2007, p. 341.